IAI Journals.ASM.org

Yersinia pseudotuberculosis Efficiently Escapes Polymorphonuclear Neutrophils during Early Infection

Linda Westermark,[a,b,c] Anna Fahlgren,[a,b] Maria Fällman[a,b,c]

Department of Molecular Biology,[a] Umeå Centre for Microbial Research (UCMR),[b] and Laboratory for Molecular Infection Medicine Sweden (MIMS),[c] Umeå University, Umeå, Sweden

The human-pathogenic species of the Gram-negative genus *Yersinia* preferentially target and inactivate cells of the innate immune defense, suggesting that this is a critical step by which these bacteria avoid elimination and cause disease. In this study, bacterial interactions with dendritic cells, macrophages, and polymorphonuclear neutrophils (PMNs) in intestinal lymphoid tissues during early *Yersinia pseudotuberculosis* infection were analyzed. Wild-type bacteria were shown to interact mainly with dendritic cells, but not with PMNs, on day 1 postinfection, while avirulent *yopH* and *yopE* mutants interacted with PMNs as well as with dendritic cells. To unravel the role of PMNs during the early phase of infection, we depleted mice of PMNs by using an anti-Ly6G antibody, after which we could see more-efficient initial colonization by the wild-type strain as well as by *yopH*, *yopE*, and *yopK* mutants on day 1 postinfection. Dissemination of *yopH*, *yopE*, and *yopK* mutants from the intestinal compartments to mesenteric lymph nodes was faster in PMN-depleted mice than in undepleted mice, emphasizing the importance of effective targeting of PMNs by these *Yersinia* outer proteins (Yops). In conclusion, escape from interaction with PMNs due to the action of YopH, YopE, and YopK is a key feature of pathogenic *Yersinia* species that allows colonization and effective dissemination.

The Gram-negative bacterial genus *Yersinia* includes three human-pathogenic species. *Yersinia pestis* is the causative agent of plague, and *Yersinia pseudotuberculosis* and *Yersinia enterocolitica* cause gastroenteritis. Enteric *Yersinia* infections are characterized by fever, abdominal pain, and diarrhea and are usually self-limiting in humans. An oral infection model for these pathogens in mice mimics the human enteric infection. Depending on the bacterial infection dose, clearance, systemic disease, and persistent infection can be studied in mice (1–3; A. Fahlgren et al., unpublished data). *Yersinia* is an extracellular pathogen that can survive and proliferate in lymphoid tissue (4). Infection with enteric *Yersinia* species occurs via the oral route, and the bacteria enter the intestinal tissue through invasion of M cells, present in the intestinal follicle-associated epithelium. During the first stages of infection, bacteria are localized in the Peyer's patches (PPs) of the small intestine and the lymphoid follicles of the cecum (3). At these locations, *Yersinia* encounters innate immune cells, including resident dendritic cells (DCs) and macrophages. Polymorphonuclear neutrophils (PMNs) are also recruited to the site of infection to help eliminate the invading bacteria (3, 5–8).

PMNs are the third most abundant type of leukocyte in mouse blood, after B and T lymphocytes (9). These blood-circulating phagocytes have a short life span (12 h) and are continuously replenished from bone marrow (10, 11). Upon infection by invading microorganisms, PMNs play a fundamental role in the primary innate immune defense and use several mechanisms for the elimination of bacteria, such as phagocytosis, degranulation, and neutrophil extracellular trap (NET) formation (12). PMNs have been shown to be important for controlling enteric *Yersinia* infections (13, 14). *Yersinia* species target primarily PMNs, but also DCs and macrophages, through the transfer of *Yersinia* outer proteins (Yops) into these cells via the type three secretion system (T3SS) (13, 15–17), thus indicating that avoidance of the action of all these immune cells is important for successful infection. Upon delivery into PMNs, the Yop effectors can inhibit phagocytosis, the production of reactive oxygen species, and NET formation (18–20). The YopH and YopE effectors have been identified as major contributors to the antiphagocytic capacity of *Y. pseudotuberculosis* against macrophages and PMNs (21–24). YopH interrupts early signaling events from the phagocytic receptor, while YopE blocks actin dynamics. In contrast, blocking internalization by DCs requires only YopE, a phenomenon that can be explained by the fact that these cells do not use strictly receptor mediated mechanisms for the internalization of antigens (21). Antiphagocytosis is likely an essential virulence mechanism of *Yersinia*, and virulence studies in mice further support this hypothesis, since *yopH* and *yopE* single mutants are cleared at early stages of infection (25). A *yopH* mutant is usually cleared at the level of PPs and a *yopE* mutant in the mesenteric lymph nodes (MLNs). YopH is a powerful tyrosine phosphatase and has been shown to act on proteins associated with signaling from the β1-integrin receptor, where the molecular targets differ depending on the cell type. The targets identified so far are focal adhesion kinase (FAK) and p130Cas in HeLa cells (26–28), the immune cell-specific protein Fyn-binding protein (Fyb; also called ADAP and SLAP-130) and SKAP-HOM in macrophages (26, 29), and SLP-76 and SKAP-HOM in PMNs (30). YopE has GTPase-activating protein (GAP) activity and has been shown to inactivate Rho-family GTPases (31–33). The Rho-family GTPases participate in the control of many cellular functions, such as the regulation of actin dynamics in eukaryotic cells (34).

Received 19 December 2013 **Accepted** 19 December 2013
Published ahead of print 30 December 2013
Editor: A. J. Bäumler
Address correspondence to Maria Fällman, maria.fallman@molbiol.umu.se.
Supplemental material for this article may be found at http://dx.doi.org/10.1128/IAI.01634-13.

doi:10.1128/IAI.01634-13

In the present study, we aimed to investigate bacterium-immune cell interactions and their effects during initial colonization in intestinal lymphoid compartments and, in particular, to study the role of PMNs. Depletion of PMNs in mice with antibodies is a commonly used approach to reveal the role and importance of PMNs. Two depletion antibodies are available, and both recognize glycoproteins on the cell surface, but with different specificities. Anti-Ly6G is considered to deplete PMNs specifically, since it binds only to Ly6G (35). Anti-Gr-1 recognizes both Ly6G and Ly6C and therefore depletes monocytes in addition to PMNs (36). These antibody depletion models have been used previously to study the role of PMNs during infections with wild-type (wt) bacteria of different *Yersinia* species and with certain *yop* mutants (14, 20, 37, 38). In a recent study, we showed that depletion of Gr-1$^+$ cells enables the otherwise avirulent *Y. pseudotuberculosis yopK* mutant to cause systemic infection in mice (20). Further, *Y. pestis* grows better in the spleen and liver upon depletion of Gr-1$^+$ cells, and a *Y. pestis yopM* mutant is more virulent after depletion of either Gr-1$^+$ or Ly6G$^+$ cells (37, 38). However, the effects of PMN depletion on early infection have not been investigated previously.

We show that *Y. pseudotuberculosis* interacts with DCs in PPs and cecal lymphoid follicles during early infection (day 1 postinfection [p.i.]). However, in contrast to wt bacteria, avirulent *yopH* and *yopE* mutants also interact with recruited PMNs at this time point. In a previous study using the CD11c-DTR model for depletion of DCs, we could not show an obvious role of DCs during the establishment of *Y. pseudotuberculosis* infection (39). In the current study, we therefore focused on the role of PMNs during early infection. By depletion of PMNs using an anti-Ly6G antibody, we show that PMNs are important for the restriction of *yopH*, *yopE*, and *yopK* mutants during the initial stages of infection. In the absence of PMNs, these mutants are disseminated more efficiently from the intestinal tissue to MLNs. Our study reveals the role and significance of the *Y. pseudotuberculosis* resistance to PMNs and shows that the different Yop effectors together contribute to the extensive capacity of this pathogen to circumvent these efficient bacterial eliminators.

MATERIALS AND METHODS

Mice. Eight-week-old female BALB/c mice were purchased from Taconic, Denmark, and were given food and water *ad libitum*. The study was approved by the local animal ethics committee (Dnr A90-11 and A192-12).

Bacteria. For animal experiments, the following bioluminescent *Y. pseudotuberculosis* strains harboring the *Photorhabdus luminescens luxCDABE* operon integrated on the virulence plasmid were used: the wt strain YPIII(pCD1, Xen4) (Caliper Life Sciences) and the corresponding *yopH* [YPIII(pCD30, Xen4)], *yopE* [YPIII(pCD526, Xen4)] (40), and *yopK* [YPIII(pCD155, Xen4)] (41) deletion mutants. The wt strain [YPIII(pCD1, Xen4)] was used to create the bioluminescent *yopH* deletion mutant [YPIII(pCD30, Xen4)] by amplifying DNA fragments flanking the gene to be deleted. A secondary PCR using the flanking-region products as templates was performed, and the product was cloned into the suicide vector pDM4 (40), which was then introduced into YPIII(pCD1, Xen4) by conjugational mating using *Escherichia coli* S17-1 *pir* as the donor strain. Integration of mutations formed by homologue recombination and subsequent segregation was done using established methods (40). The *yopH* mutant was confirmed by sequencing.

Mouse infections. For oral infection, the mice were deprived of food and water for 16 h prior to infection. Bacterial suspensions were prepared by growing bacteria overnight in LB medium at 26°C, followed by resuspension in sterile tap water supplemented with 150 mM NaCl. The mice were allowed to drink the bacterial suspensions for 6 h, after which food and water were returned. Infection doses were determined by CFU counts of serially diluted bacterial cultures used for infection in combination with measurement of drinking volumes and found to be 2.9×10^8 to 6.3×10^8 CFU/mouse.

Flow cytometry to monitor PMN depletion and immune response. To deplete PMNs, mice were injected intraperitoneally with 100 μg of the monoclonal anti-Ly6G antibody (clone 1A8; BioXCell) diluted in 100 μl sterile phosphate-buffered saline (PBS) 1 day before infection and 2 days postinfection (p.i.). Mice injected with 100 μl sterile PBS served as controls. To ensure that Ly6G$^+$ cells had been depleted and to monitor Gr-1$^+$ cells, flow cytometric analysis of mouse blood was performed at days 1, 3, and 5 p.i. Briefly, whole blood from the mouse tail vein was collected in an equal volume of PBS supplemented with 10% fetal calf serum, 0.002% NaN_3, and heparin. Erythrocytes were removed by treatment with a lysis buffer containing 0.15 M NH_4Cl, 10 mM K_2CO_3, and 0.1 mM EDTA, followed by centrifugation. The remaining leukocytes were stained with phycoerythrin (PE)- or fluorescein isothiocyanate (FITC)-conjugated anti-Gr-1 (clone RB6-8C5; eBioscience) and with a PE- or allophycocyanin (APC)-conjugated antibody against major histocompatibility complex class II (MHC-II) (clone M5/144.15.2; BD Biosciences and eBioscience). To further monitor the immune response to the infection, blood leukocytes were stained with APC-conjugated anti-Gr-1 (clone RB6-8C5; eBioscience) and PE-conjugated anti-F4/80 (clone BM8; eBioscience). Corresponding isotype controls were used as negative controls (eBioscience). Flow cytometry was performed using a FACSCalibur flow cytometer (Becton, Dickinson).

Monitoring of infection by IVIS. Infection was monitored and analyzed by *in vivo* imaging systems (IVIS), using IVIS Spectrum (Caliper Life Sciences). Mice were anesthetized with 2.5% isoflurane (IsoFlo Vet; Orion Pharma) and thereafter were placed in the IVIS imaging chamber (Caliper Life Sciences) under 0.5% isoflurane anesthesia. The total photon emissions from the bioluminescent bacteria inside the mice or from dissected organs were acquired for 10 to 120 s. Acquired images were analyzed by Living Image software, version 3.1 (Caliper Life Sciences). The bioluminescent signals emitted by the bacteria were determined from a set of regions of interest (ROIs) on the abdominal side of each mouse and expressed as total flux (photons per second).

Immunofluorescence. PPs, ceca, and MLNs were freshly frozen on isopentane prechilled on liquid nitrogen and were kept at −80°C. Cryosections (10 μm) of the tissues were fixed with 4% paraformaldehyde in PBS and were permeabilized with 0.5% Triton X-100 (Amersham Biosciences). To block nonspecific binding, the specimens were overlaid with 0.1 M glycine, avidin/biotin block if needed (Vector Laboratories), 1% bovine serum albumin (Boehringer Mannheim, GmbH, Germany) in PBS, and 5% serum from the secondary-antibody host. For interaction studies, double immunofluorescent staining of the sections was performed. First, the sectioned tissues were stained for the immune cell of interest, with either anti-CD11c (clone N418; eBioscience), anti-F4/80 (clone BM8; eBioscience), or anti-Ly6G (clone 1A8; BD Biosciences) and a secondary antibody conjugated with biotin (either a biotin-conjugated goat anti-Armenian hamster antibody or a biotin-conjugated mouse anti-rat antibody [both from Jackson ImmunoResearch]), followed by Alexa Fluor 555-labeled streptavidin (Invitrogen). Then sections were incubated with anti-*Yersinia* serum and an Alexa Fluor 488-labeled donkey anti-rabbit secondary antibody. For *Yersinia* staining, only the second step of the staining was performed. For the identification of inflammatory macrophages, double immunofluorescent staining with anti-F4/80 (clone BM8; eBioscience) and an Alexa Fluor 546-labeled goat anti-rat secondary antibody (Invitrogen) was combined with biotinylated anti-Ly6C (clone HK1.4; BioLegend), followed by FITC-labeled streptavidin (eBioscience). Control staining using isotype control antibodies or only secondary antibodies was performed for all analyses. Finally, 4′,6-diamidino-2-phenylindole (DAPI) was used to stain the nuclei. The specimens were mounted in Mowiol (Calbiochem). The stained sections were examined with a Nikon Eclipse 90i microscope, and images were captured using a

Hamamatsu Orcha C4742-95 camera and NIS-Elements AR 3.2 software (Nikon Instruments). For confocal microscopy, stained sections were examined in a C1 confocal scanner mounted on a Nikon Eclipse 90i microscope with EZ-C1 3.91 operating software (Nikon Instruments).

Immunohistochemistry. PPs, ceca, and MLNs were freshly frozen on isopentane prechilled on liquid nitrogen and were kept at −80°C. Ten-micrometer cryosections of the tissues were fixed with 4% paraformaldehyde in PBS. Nonspecific binding was blocked with 0.1 M glycine; endogenous peroxidase was blocked by incubation in PBS with 2 mM NaN_3 and 0.03% H_2O_2 at 37°C; and endogenous biotin was blocked with avidin/biotin treatment (Vector Laboratories). Further, unspecific binding was blocked with 0.2% bovine serum albumin (BSA; Boehringer Mannheim) in PBS. The sections were incubated with hamster anti-mouse CD11c (clone N418; AbD Serotec), rat anti-mouse Ly6G (clone 1A8; BD Biosciences Pharmingen), rat anti-mouse Gr-1 (clone RB6-8C5; BD Biosciences Pharmingen), or rat anti-mouse F4/80 (clone CI:A3-1; AbD Serotec) in 0.2% BSA. Armenian hamster IgG (Serotec) and rat IgG2b (Serotec) were used as isotype controls. A biotinylated goat anti-Armenian hamster antibody or a biotinylated mouse anti-rat antibody (both from Jackson ImmunoResearch) was used as a secondary antibody, and the signal was amplified with a Vectastain ABC enhancement kit (Vector Laboratories Inc., Burlingame, CA, USA) and was developed with 3,3-diaminobenzidine (Fast DAB tablet sets; Sigma). Finally, the tissue sections were stained with methyl green (Sigma) and were mounted in Canada balsam (Sigma). The stained sections were examined with a Nikon 90i microscope, and images were captured using a Nikon DS-Fi1 camera and Nis-Elements AR software.

Statistical analysis. All analyses were performed using GraphPad Prism, version 5. Differences were analyzed by the Mann-Whitney U test, the unpaired Student *t* test, or Fisher's test, with significance set at *P* values of <0.05 (*), <0.01 (**), or <0.001 (***). Error bars in graphs correspond to the standard errors of the means or standard deviations (SD) as indicated in the figure legends.

RESULTS

***Y. pseudotuberculosis yopH* and *yopE* mutants, but not the wt strain, interact with PMNs during early infection.** In a previous study, we discovered that the antiphagocytic effector YopH does not contribute to antiphagocytosis against DCs and suggested that this Yop effector is particularly important against the more-efficient professional phagocytes, PMNs and macrophages (21). To investigate this cell type-specific feature further, an *ex vivo* interaction assay, studying the interactions of wt *Y. pseudotuberculosis* and the *yopH* and *yopE* mutants with different phagocytic cells during early infection, was performed. Mice were infected with bioluminescent bacteria and were sacrificed 1 and 3 days p.i. PPs and ceca positive for bacterial signals by *in vivo* biophotonic imaging (IVIS Spectrum) were collected, and areas with bacteria were analyzed for bacterial interactions with DCs, macrophages, and PMNs. Double immunofluorescence staining of *Yersinia* in combination with staining of DCs, macrophages, or PMNs was performed on consecutive tissue sections. During initial *Yersinia* infection (day 1 p.i.), the number of infected PPs was very low, especially for avirulent mutants (data not shown). In contrast, we observed that bacteria (including *yopH* and *yopE* mutants) almost always colonize the cecum at early time points. The structures of PPs and the lymphoid follicles of the cecum are similar, and since the first analysis of bacterium-phagocyte interactions in the PPs and ceca of wt-infected mice yielded identical results for the two tissues (data for PPs not shown), the cecum was chosen for further analyses of bacterium-immune cell interactions. In the interaction analyses, single bacteria located in the infected ceca were analyzed, because these represent direct interaction with the phagocytes. Bacterial foci were also analyzed but were not included in the data presented here, because DCs, macrophages, and PMNs were always found in close proximity to the bacterial foci, making analysis of interactions more complicated. Consequently, the percentage of interaction was determined as the percentage of bacteria that interacted with the cell type analyzed [(number of bacteria interacting with phagocytes/total number of bacteria in all tissue sections) × 100]. Since staining was executed on constitutive sections, we cannot exclude the possibility that one bacterium interacted with more than one immune cell.

Analysis of bacterium–immune-cell interactions in the infected tissues showed that wt *Y. pseudotuberculosis* interacted mainly with DCs at day 1 p.i. (Fig. 1A and C). Forty-six percent of the wt bacteria in the lymphoid follicles of the cecum interacted with DCs, and the majority of the interactions (60%) were seen in the subepithelial dome area, which is located underneath the epithelium, facing the intestinal lumen. Wt bacteria also interacted with macrophages, but to a much lower extent (4% interaction), and here all interactions were seen in the dome area. However, the wt strain did not interact with the low numbers of PMNs recruited at day 1 p.i. As infection progressed, and high numbers of PMNs were recruited to the site of infection by day 3 p.i., interactions with these cells also occurred, at a level of 45% (Fig. 1B). At this time point, interactions with DCs and macrophages were still at levels similar to those observed for day 1 p.i., 48% and 8%, respectively.

Interestingly, in contrast to wt bacteria, mutants lacking one of the antiphagocytic Yop effectors (YopH or YopE) interacted not only with DCs on day 1 p.i. (38% interaction for both the *yopH* and the *yopE* mutant), but also with PMNs, to a high extent (33% interaction for the *yopH* mutant and 68% interaction for the *yopE* mutant) (Fig. 1A and C). This discrepancy with the wt strain in PMN interaction could not be explained by a difference in PMN recruitment between the different bacterial strains (see Fig. S1 in the supplemental material). Also, at day 3 p.i., the levels of interaction of mutant bacteria with both DCs and PMNs were significantly higher than those for wt bacteria. The percentages of interaction with DCs were 81% for the *yopH* mutant and 82% for the *yopE* mutant (compared with 48% for the wt). At this time point, 100% of the *yopH* mutant bacteria and 99% of the *yopE* mutant bacteria interacted with PMNs (compared with 45% for the wt) (Fig. 1B). Interestingly, interactions with PMNs occurred more frequently in the subepithelial dome for the *yop* mutants than for the wt strain, where such interactions were mainly found deeper in the tissue (30% of all wt interactions, 74% of all *yopH* mutant interactions, and 77% of all *yopE* mutant interactions were in the dome area). It is noteworthy that fewer single bacteria of the *yopH* mutant (1.5 ± 0.6 bacteria/section) or the *yopE* mutant (2.2 ± 1.5 bacteria/section) than of the wt strain (4.4 ± 3.1 bacteria/section) could be found in the sectioned tissues at day 1 p.i. The average numbers of single bacteria per microcolony detected at day 1 p.i. were 4.1 for the wt, 5.8 for the *yopH* mutant, and 3.7 for the *yopE* mutant, as determined from sets of three centrally located sections from IVIS-positive cecal lymphoid follicles. In addition, lower percentages of total bacteria had passed the subepithelial dome and entered further into the lymphoid follicle for the *yopH* (34%) and *yopE* (14%) mutants than for the wt strain (51%), indicating that wt bacteria disseminate faster through the lymphoid tissues than *yopH* and *yopE* mutant bacteria.

To investigate the interaction of *Y. pseudotuberculosis* with

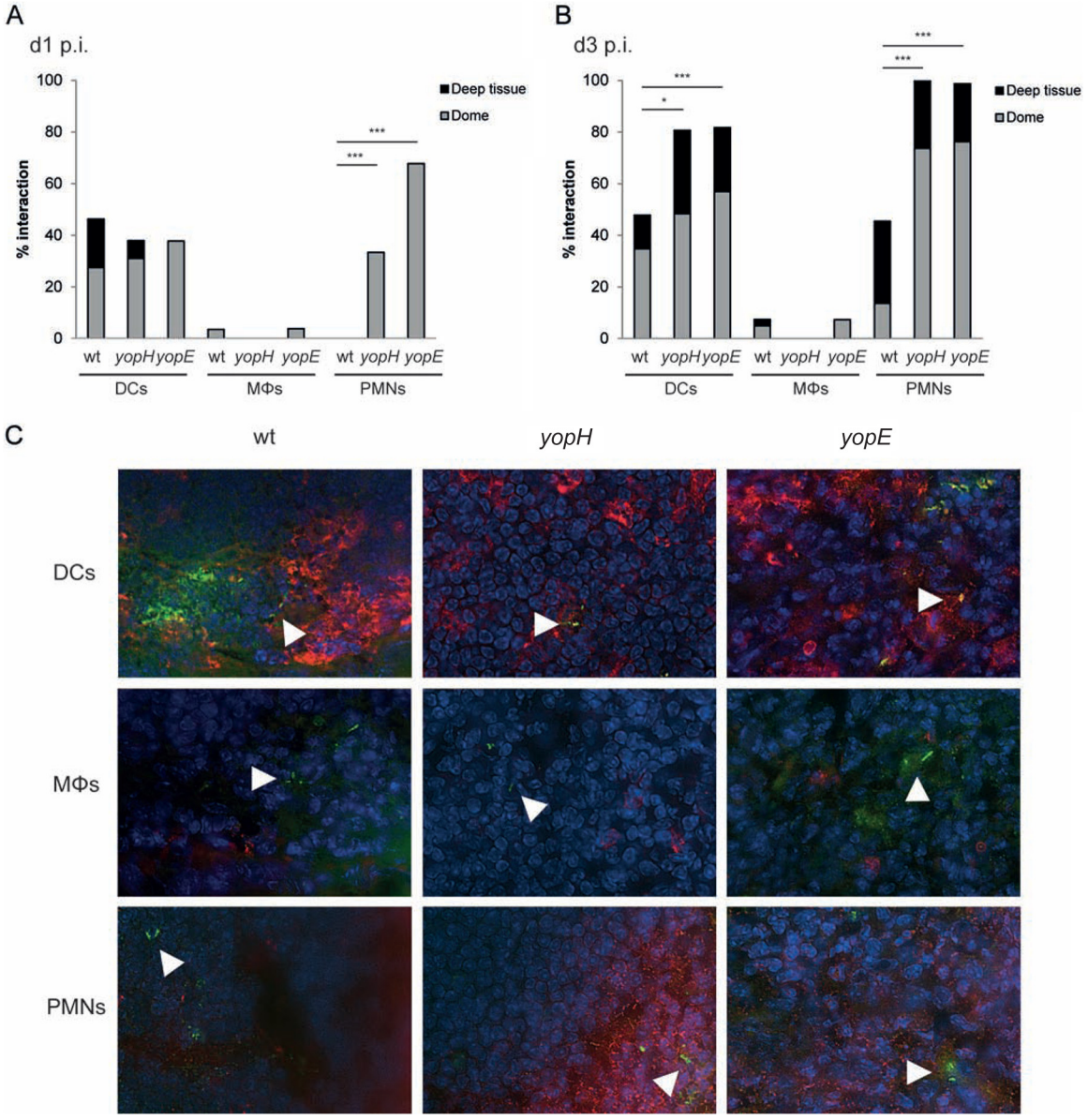

FIG 1 Avirulent Yop mutants, but not wild-type *Y. pseudotuberculosis*, interact with PMNs during early infection. BALB/c mice were infected with wt bioluminescent *Y. pseudotuberculosis* or a *yopH* or *yopE* mutant. At 1 and 3 days postinfection, ceca positive for bacterial signals by IVIS were collected. Tissues were cryosectioned and were stained for bacteria in combination with staining for dendritic cells (DCs), macrophages (Mϕs), or neutrophils (PMNs). Stained ceca were analyzed by microscopy, and each bacterium observed was calculated as one event. Bacterial foci were not included in the analysis. (A) Percentage of bacteria interacting with immune cells in the subepithelial dome and the whole lymphoid follicle at day 1 (d1) p.i. Data for wt *Y. pseudotuberculosis* represent 15 sections per staining from 7 to 8 mice; data for the *yopH* mutant represent 16 to 21 sections per staining from 8 to 10 mice; and data for the *yopE* mutant represent 12 to 20 sections per staining from 4 to 7 mice. Differences between groups were analyzed by Fisher's test, with significance set at P values of <0.05 (*), <0.01 (**), or <0.001 (***). (B) Percentage of bacteria interacting with immune cells in the subepithelial dome and the whole lymphoid follicle at day 3 p.i. Data for wt *Y. pseudotuberculosis* represent 8 to 11 sections per staining from 4 to 5 mice; data for the *yopH* mutant represent 7 to 9 sections per staining from 4 mice; and data for the *yopE* mutant represent 4 to 5 sections per staining from 4 to 5 mice. (C) Representative images of bacteria interacting (or not) with DCs, Mϕs, or PMNs in lymphoid follicles of the cecum at day 1 p.i. White arrowheads indicate single bacteria.

phagocytes further, we also analyzed extracellular versus intracellular localization of the stained bacteria by confocal microscopy. Wt bacteria were shown to be predominantly extracellular in their interaction with DCs at day 1 p.i. (67%). Interestingly, the *yopH* and *yopE* mutants were also predominantly extracellular at day 1 p.i. in their interactions both with DCs (78% for the *yopH* mutant and 76% for the *yopE* mutant) and with PMNs (70% for the *yopH* mutant and 92% for the *yopE* mutant). Thus, the increased percentages of interaction of the *yopH* and *yopE* mutants with PMNs cannot be explained by a degree of internalization higher than that of the wt. However, these data do not reveal whether the mutant bacteria are alive or have been killed by other antimicrobial actions.

Taken together, the data suggest that wt *Yersinia*, in contrast to the avirulent *yopH* and *yopE* mutants, avoids stable interaction with PMNs during the initial stages of infection. Further, the data

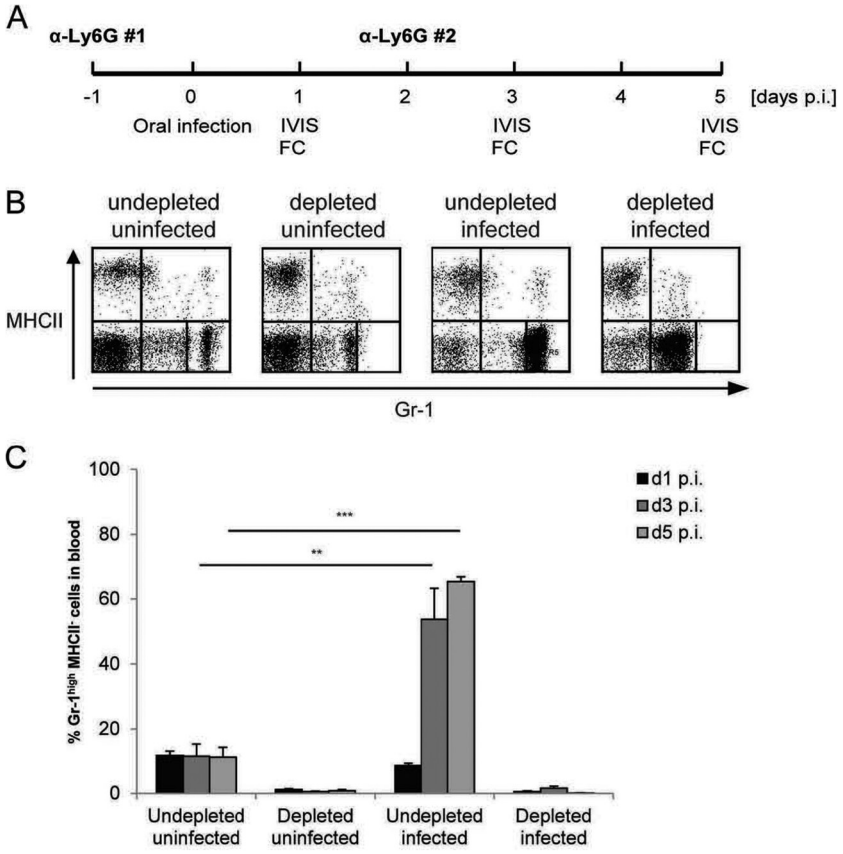

FIG 2 *Y. pseudotuberculosis* infection results in increases in the numbers of Gr-1^{high} MHC-II^{-} cells in the blood of undepleted mice but not in the blood of PMN-depleted mice. BALB/c mice were depleted of PMNs by intraperitoneal injections of an anti-Ly6G antibody and were infected with bioluminescent *Y. pseudotuberculosis*. Mice injected with PBS served as controls. (A) Time line over the experimental setup. IVIS, *in vivo* imaging system; FC, flow cytometry. (B) Representative dot plots from flow cytometry analysis of PMN depletion, performed on blood from undepleted and depleted uninfected control mice and wt-infected mice. Blood leukocytes were isolated and were analyzed for the expression of Gr-1 and MHC-II. PMNs were identified as Gr-1^{high} MHC-II^{-} cells (lower far right quadrants). (C) Flow cytometry analysis of PMN depletion. Blood from undepleted and depleted mice, either uninfected or infected with wt *Y. pseudotuberculosis*, was collected on days 1, 3, and 5 p.i., and cellular expression of Gr-1 and MHC-II was determined by flow cytometry analysis. Data for gated Gr-1^{high} MHC-II^{-} cells are presented as means ± SD. Differences between groups were analyzed by an unpaired Student *t* test, with significance set at *P* values of <0.05 (*), <0.01 (**), or <0.001 (***).

indicate that the early interaction between PMNs and the *yop* mutants might be a reason for their avirulence in mice.

PMN depletion results in increased levels of initial bacterial colonization. To further investigate the role of PMNs during early *Yersinia* infection and the role of these cells in the restriction and avirulence of *yopH* and *yopE* mutants, we used conditional PMN depletion *in vivo* by treatment of mice with the anti-Ly6G antibody. BALB/c mice were injected with anti-Ly6G, or with sterile PBS as a control, 1 day before and 2 days after oral infection with 10^8 CFU/ml of bioluminescent wt or *yopH*, *yopE*, or *yopK* mutant bacteria. The *yopK* mutant was included as a control, since a previous study had shown that its virulence increased upon depletion of Gr-1^{+} cells, suggesting a role for PMNs in the restriction of infection (20). The experimental setup included flow cytometry of stained blood cells to monitor depletion and *in vivo* biophotonic imaging using the IVIS Spectrum system to monitor infection at days 1, 3, and 5 p.i. (Fig. 2A). Additionally, the mice were examined for physical disease symptoms, and five mice from each group were sacrificed and dissected in order to analyze bacterial dissemination by IVIS.

Physical examinations of the mice for disease symptoms such as ruffled fur, diarrhea, hunchback posture, and inactivity were performed daily throughout the experiment. At day 3 p.i., PMN-depleted mice infected with wt bacteria showed somewhat more disease symptoms than undepleted mice infected with wt bacteria (Table 1). However, at the termination of the experiment on day 5 p.i., these two groups of wt-infected mice showed similar degrees of disease symptoms. PMN-depleted mice infected with the *yopE* mutant showed symptoms of disease at days 3 and 5 p.i., whereas the corresponding undepleted mice were totally symptom free during the entire infection period. As with the wt strain, PMN-depleted mice infected with the *yopK* mutant showed more-severe disease symptoms than undepleted mice, but at day 5 p.i., the two groups of *yopK*-infected mice showed the same level of disease symptoms. Mice infected with the *yopH* mutant were symptom free throughout the infection, regardless of PMN depletion. Thus, depletion of PMNs using the anti-Ly6G antibody resulted in more-severe symptoms of disease and a faster spread of infection compared to the situation in undepleted mice.

To monitor PMN depletion, blood was collected on days 1, 3, and 5 p.i. from uninfected control mice and wt-infected mice treated with PBS or anti-Ly6G, and flow cytometry was used to

TABLE 1 Visual physical examination of disease symptoms

Day p.i.	Disease symptoms[a] in uninfected mice		Disease symptoms[a] in mice infected with:							
			wt		*yopH* mutant		*yopE* mutant		*yopK* mutant	
	Undepleted	Depleted[b]	Undepleted	Depleted	Undepleted	Depleted	Undepleted	Depleted	Undepleted	Depleted
1	−	−	−	−	−	−	−	−	−	−
3	−	−	+	++	−	−	−	+	−	+
5	−	−	++	++	−	−	−	+	+	+

[a] −, healthy mice with no signs of disease; +, initial symptoms of disease, i.e., ruffled fur; ++, symptoms of disease, i.e., ruffled fur, diarrhea, and hunchback posture; +++, severe symptoms of disease, i.e., ruffled fur, diarrhea, hunchback posture, and inactivity.
[b] "Depleted" mice were depleted of PMNs by treatment with an anti-Ly6G antibody.

analyze the expression of Gr-1 (Ly6G/C) and major histocompatibility complex class II (MHC-II) on isolated blood leukocytes. This combination of antibodies was used both to detect and to separate PMNs and monocytes. Uninfected, undepleted control mice had stable levels of Gr-1^{high} MHC-II^{-} cells (corresponding to PMNs), ranging from 11.3% to 11.8%, during the whole experimental period (Fig. 2B, lower far-right quadrant, and C). In contrast, for wt-infected, undepleted mice, the level of Gr-1^{high} MHC-II^{-} cells in blood increased during infection, from 8.8% ± 0.6% on day 1 p.i. to 53.7% ± 9.8% on day 3 p.i. and 65.5% ± 1.5% on day 5 p.i. (Fig. 2C). Thus, wt *Y. pseudotuberculosis* infection results in a gradual increase in the level of PMNs in the blood. Ly6G-treated mice, both uninfected and wt infected, were depleted of Gr-1^{high} MHC-II^{-} cells and thus had low levels of PMNs in the blood throughout the experiment, ranging from 0.6% to 1.2% and 0.6% to 1.6%, respectively (Fig. 2B and C). Thus, the amount of anti-Ly6G injected was sufficient to deplete Gr-1^{high} MHC-II^{-} cells in blood both at steady state and during *Y. pseudotuberculosis* infection.

To determine the level of bacterial infection, the infected mice were anesthetized, and bioluminescent signals from the infecting bacteria were measured by IVIS. The IVIS analysis suggested higher levels of colonization with all bacterial strains for PMN-depleted mice than for undepleted mice at day 1 p.i. (Fig. 3). For wt-infected mice, the bacterial signal was four times higher in PMN-depleted mice than in undepleted mice (19.0×10^7 versus 5×10^7 photons s^{-1}). The signal was three times higher for depleted *yopH* mutant-infected mice (6.6×10^7 versus 2.6×10^7 photons s^{-1}), four times higher for depleted *yopE* mutant-infected mice (6.1×10^7 versus 1.6×10^7 photons s^{-1}), and two times higher for *yopK* mutant-infected mice (9.1×10^7 versus 3.9×10^7 photons s^{-1}) (Fig. 3B). Thus, the data indicate that PMN depletion leads to an increased level of initial infection with *Y. pseudotuberculosis*. Surprisingly, this difference in bacterial signals was not observed at days 3 and 5 p.i., when the levels of bacterial signals in PMN-depleted mice were similar to those in undepleted mice or, in some cases, even lower (Fig. 3). Noteworthy, at later stages of infection, the relative signal strengths do not depend solely on bacterial counts, since bacterial dissemination into deeper tissue can also result in less external signal. At day 3 p.i., for example, the signals from PMN-depleted mice infected with wt bacteria were lower than those from undepleted wt-infected mice, although according to physical examinations, the PMN-depleted mice showed much more severe disease symptoms.

Faster dissemination of avirulent *yop* mutants to MLNs in the absence of PMNs. Next, bacterial dissemination was investigated by dissection of five mice from each of the eight infection groups, i.e., undepleted or PMN-depleted mice infected with wt, *yopH*, *yopE*, or *yopK* bacteria. The bioluminescent signals from individual organs were measured by IVIS. For wt bacteria, PMN depletion had no effect on dissemination to MLNs at day 1 p.i.; there was no difference in the number of infected MLNs between undepleted and PMN-depleted mice (Fig. 4). For both groups, bacteria had disseminated from PPs to MLNs in 3 of 5 mice. In contrast, levels of dissemination of all *yop* mutants were already clearly higher in the absence of PMNs on day 1 p.i. (Fig. 4). For the *yopH* mutant, no dissemination to MLNs could be observed in undepleted mice, while 3 of 5 PMN-depleted mice had bacteria in the MLNs. The *yopE* mutant showed increased dissemination capacity, from 1 of 5 undepleted mice to 4 of 5 PMN-depleted mice with infected MLNs. The *yopK* mutant showed a similar pattern in its capacity of dissemination to MLNs, from 2 of 5 undepleted mice to 4 of 5 PMN-depleted mice. The increased dissemination to MLNs observed in the absence of PMNs correlated well with the disease symptoms: the individual mice that showed signs of disease also had bioluminescent signals in MLNs, whereas mice that appeared healthy also lacked signals.

The analysis of dissemination at days 3 and 5 p.i. confirmed the results from the measurement of total external IVIS signals for the same days (Fig. 3), showing no obvious differences between undepleted and PMN-depleted mice (data not shown). Only one exception was observed: among *yopH* mutant-infected mice at day 5 p.i., 1 of 5 undepleted mice had signals in their MLNs compared to 3 of 5 PMN-depleted mice. This finding likely reflects efficient clearing of this mutant from the PPs by PMNs in undepleted mice.

Taken together, these results show that during the initial stage of infection, the otherwise avirulent *yopH*, *yopE*, and *yopK* mutants disseminate to MLNs more efficiently in PMN-depleted mice than in undepleted mice.

Immature PMNs contribute to the final clearance of bacteria in PMN-depleted mice. The IVIS analysis of bacterial signals from mice and dissected organs showed that depletion of PMNs by injection of the anti-Ly6G antibody did not lead to higher levels of bacterial colonization and systemic spread at days 3 and 5 p.i., suggesting that perhaps other immune cells were acting in the PMN-depleted mice at later time points. Reanalysis of the flow cytometry data of PMN depletion efficiency in blood showed that the proportion of cells with intermediate expression of the PMN marker Gr-1 (Ly6G/C) and no expression of MHC-II (i.e., Gr-1^{low} MHC-II^{-} cells) increased in wt-infected PMN-depleted mice (Fig. 5A). The level of increase (from 14.3% ± 1.1% on day 1 p.i. to 33.8% ± 6.4% on day 3 p.i. and 60.5% ± 12.3% on day 5 p.i.) was similar to that observed for Gr-1^{high} MHC-II^{-} cells (PMNs) in wt-infected, undepleted mice (Fig. 2C). Hence, this Gr-1^{low}

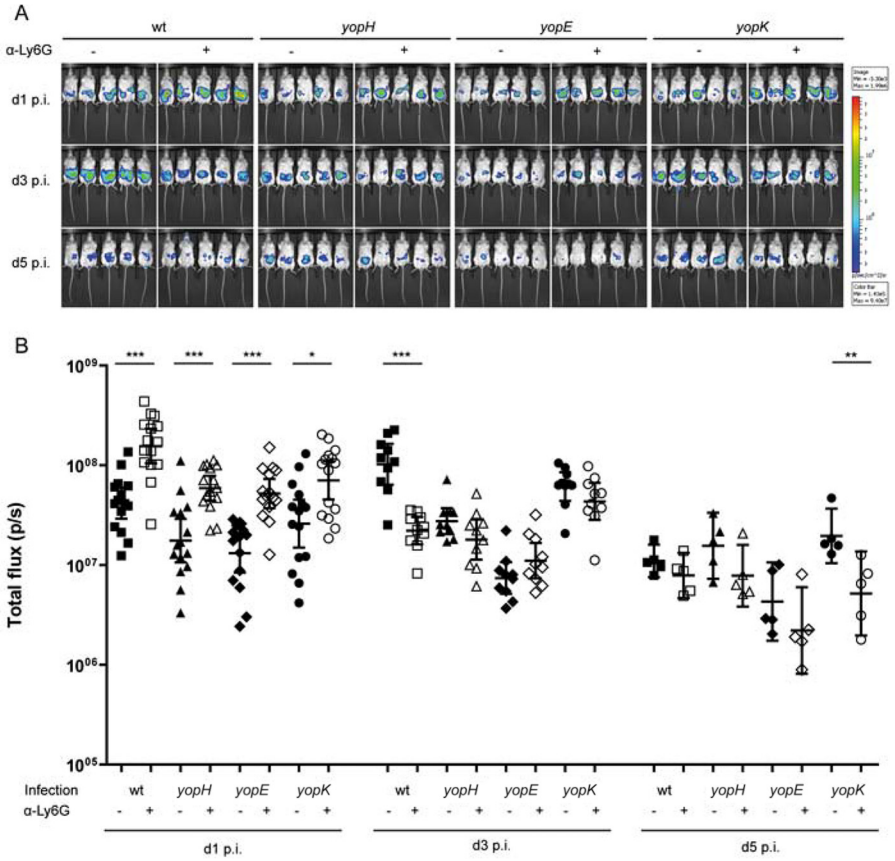

FIG 3 PMN depletion results in increased levels of initial bacterial infection. BALB/c mice were depleted of PMNs by intraperitoneal injections of an anti-Ly6G antibody and were infected with wt bioluminescent *Y. pseudotuberculosis* or with a *yopH*, *yopE*, or *yopK* mutant. Mice injected with PBS served as controls. The infection was monitored and analyzed by IVIS for 5 days. (A) Representative groups of mice followed throughout the infection are shown. The intensity of emission is represented with pseudocolors, with variations in color representing light intensity. Red represents the most intense light emission, while blue corresponds to the weakest signal. (B) Determination of signals at days 1, 3, and 5 p.i. from bioluminescent bacteria in the abdominal sides of BALB/c mice treated with PBS or anti-Ly6G. A total of 15 mice were used for day 1 p.i., 10 for day 3 p.i., and 5 for day 5 p.i., for all groups included. The bacterial signals were measured from sets of regions of interest and are presented as the geometric means of total flux (photons per second per area). Differences between groups were analyzed by the Mann-Whitney U test, with significance set at *P* values of <0.05 (*), <0.01 (**), or <0.001 (***).

MHC-II$^-$ population may compensate for the loss of PMNs in the blood of PMN-depleted mice. To investigate what type(s) of immune cell the Gr-1^{low} MHC-II$^-$ population represented, a more detailed flow cytometry analysis of blood cells was performed on samples collected at day 5 p.i. This analysis separated PMNs at different maturity states and monocytes from each other through their expression of Gr-1 and F4/80 (Fig. 5B and C). The analysis revealed that in wt-infected, undepleted mice, the major Gr-1$^+$ cell type in blood was Gr-1^{high} F4/80$^-$ cells (Fig. 5B, lower far-right quadrants), i.e., mature PMNs (56.5% ± 14.7%). In contrast, in wt-infected, PMN-depleted mice, Gr-1^{low} F4/80$^-$ cells (immature PMNs) were dominant (30.0% ± 6.9%) (Fig. 5B, lower middle quadrants). Levels of Gr-1$^+$ F4/80$^+$ monocytes also showed a slight, but not significant, increase in blood from wt-infected, PMN-depleted mice (Fig. 5B, upper right quadrants, and C). In agreement with a previous report (5), the levels of Gr-1^{high} F4/80$^-$ mature PMNs in blood at day 5 p.i. were lower in undepleted mice infected with any of the *yop* mutants than in wt-infected, undepleted mice (see Fig. S2 in the supplemental material). The level of mature PMNs in the blood of wt-infected mice was 56.5% ± 14.7%, while *yopH* mutant-infected mice had 20.5% ± 8.0%, *yopE* mutant-infected mice had 9.5% ± 2.2%, and *yopK* mutant-infected mice had 11.2% ± 2.1% mature PMNs.

Taken together, the data show that in undepleted mice, mature PMNs are the major inflammatory cells recruited upon *Y. pseudotuberculosis* infection. The level of mature PMNs in blood is higher in mice infected with wt bacteria than in mice infected with avirulent *yop* mutants. These data, together with data showing a gradual increase in the proportion of PMNs in blood during infection (Fig. 2B), and analysis of bacterial dissemination in mouse organs (Fig. 4), indicate that the increase in the proportion of PMNs in blood is a consequence of systemic spread of *Y. pseudotuberculosis*. In contrast, in PMN-depleted mice, immature PMNs are released into the blood. Our data suggest that these cells, likely together with slightly increasing monocyte numbers, are capable of establishing a defense against the infection.

To analyze the increases in the proportions of immature PMNs and monocytes in wt-infected, PMN-depleted mice further, immunohistochemistry was performed on PPs, ceca, and MLNs collected at day 3 p.i. and positive for bacterial signals in IVIS. First, *Yersinia* staining was performed to locate bacteria in the sectioned tissues. Then, to further evaluate the depletion in tissue and to

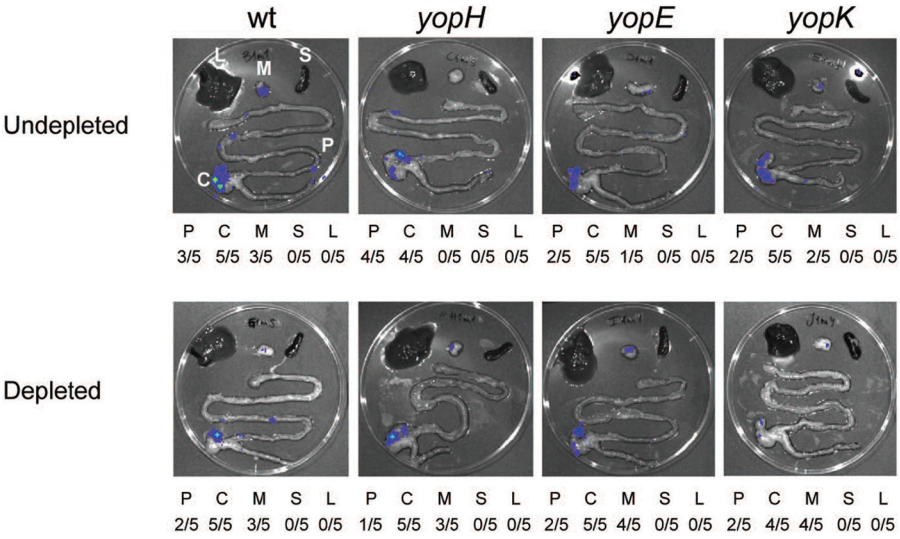

FIG 4 PMN depletion enables faster dissemination of avirulent Yop mutants to MLNs. BALB/c mice were depleted of PMNs by intraperitoneal injections of an anti-Ly6G antibody and were infected with wt bioluminescent *Y. pseudotuberculosis* or a *yopH*, *yopE*, or *yopK* mutant. Mice injected with PBS served as controls. Bacterial dissemination was determined by dissection of organs and analysis by IVIS at day 1 p.i. Pictures of organs from representative mice are presented together with the numbers of organs positive for bacterial signals by IVIS. P, Peyer's patches; C, cecum; M, mesenteric lymph node; S, spleen; L, liver.

investigate the recruitment of PMNs, monocytes, macrophages, and DCs, the tissues were stained with an anti-Ly6G, anti-Gr-1, anti-F4/80, or anti-CD11c antibody, respectively. As expected, Ly6G staining showed higher levels of PMN infiltration into the PPs, lymphoid follicles of the cecum, and MLNs of wt-infected, undepleted mice than into those of uninfected, undepleted mice on day 3 p.i. (see Fig. S3A in the supplemental material). In the tissues from wt-infected, PMN-depleted mice, Ly6G$^+$ cells were also observed (see Fig. S3A in the supplemental material), even though depletion analysis by flow cytometry showed that the blood was efficiently depleted of mature PMNs (Fig. 2B). Thus, these results supported our suggestion, based on the flow cytometry analysis, that in the absence of mature PMNs (Gr-1^{high} F4/80$^-$), immature PMNs (Gr-1^{low} F4/80$^-$) compensate for the loss by increasing in blood and also by being recruited into the infected tissues upon infection. In PMN-depleted mice, the proportion of Ly6G$^+$ cells was most prominent in PPs, which showed levels similar to those in infected, undepleted mice. In contrast, the levels of Ly6G$^+$ cells in the ceca and MLNs of PMN-depleted mice were much lower than those in PPs, and clearly lower than the levels in the corresponding tissues of undepleted mice (see Fig. S3A in the supplemental material). At day 3 p.i., the level of Ly6G$^+$ cells in tissues of PMN-depleted mice infected with the *yopH*, *yopE*, or *yopK* mutant strain was similar to that in wt-infected tissues (data not shown). Due to the infiltration of Ly6G$^+$ cells into PMN-depleted mice, Gr-1 staining could not be used to evaluate the presence of monocytes in the infected tissues as intended. However, F4/80 staining showed higher levels of macrophages in the PPs and lymphoid follicles of the ceca of infected, PMN-depleted mice than in those of undepleted mice (see Fig. S3B in the supplemental material). In MLNs, no clear difference in the number of macrophages could be observed between undepleted and PMN-depleted mice. CD11c staining showed comparable levels of DCs in infected tissues from undepleted and PMN-depleted mice (data not shown).

To further investigate the increase in the proportion of macrophages in infected tissues, PPs and lymphoid follicles of ceca from uninfected and wt-infected mice were stained for inflammatory macrophages by double immunofluorescence with anti-Ly6C and anti-F4/80 (see Fig. S4 in the supplemental material). In tissues from uninfected control mice and from wt-infected, undepleted mice on day 3 p.i., either no double-positive cells (i.e., Ly6C$^+$ F4/80$^+$ inflammatory macrophages) or very low numbers were observed. In contrast, wt-infected tissues from PMN-depleted mice contained clearly more inflammatory macrophages, confirming the results from flow cytometry analysis and immunohistochemistry. Taken together, these data suggest that in the absence of mature PMNs, the proportion of monocytes increases in blood, which also results in increased levels of inflammatory macrophages in infected tissues.

In summary, a population of Gr-1^{low} MHC-II$^-$ cells increases in the blood of PMN-depleted mice upon infection. These cells represent mainly immature PMNs, but also monocytes. Analysis by immunohistochemistry further supports this by showing that Ly6G$^+$ cells are recruited to PPs, ceca, and MLNs in PMN-depleted mice upon infection. In addition, the levels of inflammatory macrophages increase in the PPs and the lymphoid follicles of the cecum, which might be a result of monocytes entering from the bloodstream.

DISCUSSION

PMNs that are recruited to infected tissues upon infection play an important role in the defense against enteric *Yersinia* (3, 5–8, 13, 14). In this study, we show that PMNs play a fundamental role in the restriction of the initial dissemination of bacteria in intestinal tissue and that *Y. pseudotuberculosis* exhibits the capacity to efficiently escape the antimicrobial action of these normally very efficient immune cells. Using PMN-depleted mice, we show that the infection of mice with wt *Y. pseudotuberculosis* was only slightly influenced by the absence of PMNs, whereas the virulence-attenuated *yopH*, *yopE*, and *yopK* mutants were clearly more infective in the absence of these cells. Virulence capacity was evaluated

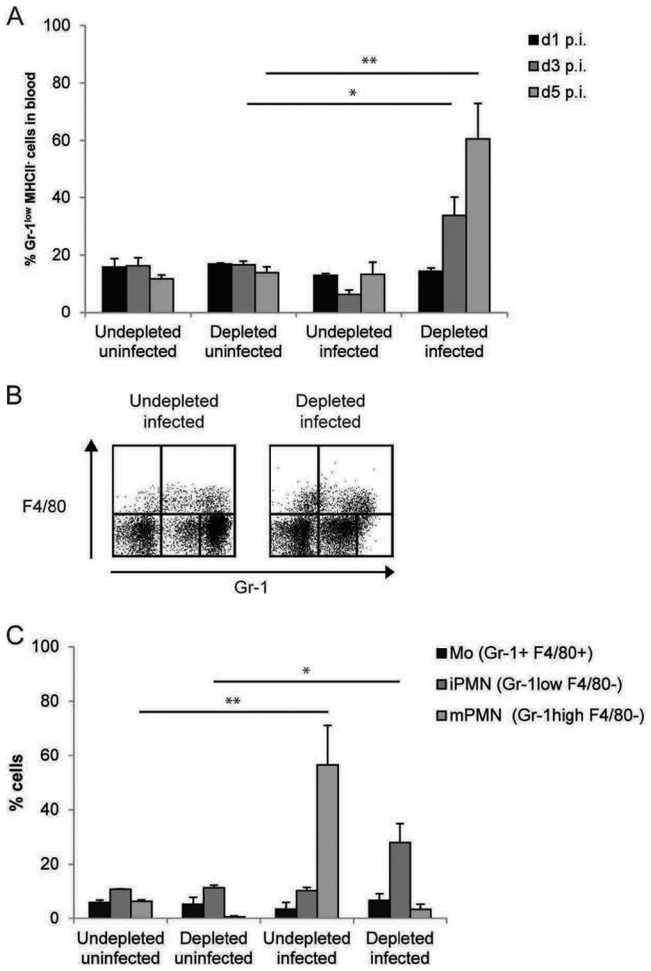

FIG 5 The proportion of Gr-1^{low} MHC-II^{-} cells increases in PMN-depleted mice infected with *Y. pseudotuberculosis*. Blood from undepleted and PMN-depleted mice, uninfected or infected with wt *Y. pseudotuberculosis*, was collected and was analyzed for the presence of Gr-1^{+} cells by flow cytometry. (A) Percentages of Gr-1^{low} MHC-II^{-} cells during the course of the experiment. Cellular expression of Gr-1 and MHC-II was determined by flow cytometry analysis. Data for gated Gr-1^{low} MHC-II^{-} cells are presented as means ± SD. (B) Representative dot plots from flow cytometry analysis performed on blood leukocytes to investigate the distribution of mature and immature PMNs and monocytes upon infection in undepleted and PMN-depleted mice. Blood leukocytes were isolated and were analyzed for the expression of Gr-1 and F4/80. Monocytes were identified as Gr-1^{+} F4/80^{+} cells (upper right quadrants), immature PMNs as Gr-1^{low} F4/80^{-} cells (lower middle quadrants), and mature PMNs as Gr-1^{high} F4/80^{-} cells (lower far right quadrants). (C) Different Gr-1^{+} cell types in blood from undepleted and depleted mice, uninfected or infected with wt *Y. pseudotuberculosis*, at day 5 postinfection. The flow cytometry analysis used gates to separate Gr-1^{+} cells into monocytes (Mo), immature neutrophils (iPMNs), and mature neutrophils (mPMNs) on the basis of their expression of Gr-1 and F4/80. Data are presented as means ± SD. Differences between groups were analyzed by an unpaired Student *t* test, with significance set at *P* values of <0.05 (*), <0.01 (**), or <0.001 (***).

using IVIS analysis of whole mice and organs as well as visual examination of signs of disease. PMN-depleted mice infected with fully virulent wt bacteria showed sickness symptoms at earlier stages of infection than undepleted mice and had higher bioluminescent signals at the first day of infection. The impact of PMNs was, however, much more obvious for the virulence-defective *yop* mutants. As seen for the wt strain, PMN-depleted mice infected with the *yopH*, *yopE*, or *yopK* mutant strain showed higher bioluminescent signals than undepleted mice infected with the same strain. Even more striking was the fact that these mutants, which normally reside in PPs and lymphoid follicles of the cecum at early phases of infection, were able to disseminate to MLNs in PMN-depleted mice already at day 1 p.i. Noteworthy, the *yopH* mutant was found in MLNs in PMN-depleted mice, even though this mutant is known to be restricted to PPs and unable to reach deeper organs (25, 42). Faster dissemination to MLNs was also reflected in the disease symptoms of PMN-depleted mice infected with the *yopE* or *yopK* mutant, which showed symptoms earlier than undepleted mice. Both the *yopE* and *yopK* mutants have been shown previously to reach MLNs before being cleared (20, 25, 42), but not at the early time points observed here in the absence of PMNs. These findings are in accordance with those of previous studies using PMN-depleted mice, showing that *Y. pseudotuberculosis yopK* and *yopH* mutants, and also *Y. pestis yopM* mutants, have higher infectious capacities in the absence of PMNs (20, 37, 38).

Taken together, our data and those of others suggest that all these Yop effectors together contribute to the PMN-resistant phenotype of *Yersinia* species and are important for the efficient escape of wt bacteria from PMNs. In this escape, YopH and YopE contribute to blockage of the signaling mediating phagocytosis and antimicrobial actions. YopK, and likely YopE, contributes to the silencing of PMN overactivation by restricting Yop delivery (31, 41, 43). The contribution of YopM to PMN resistance is less clear. This effector was recently reported to inhibit caspase-1 in macrophages (44). Caspase-1 is also active in PMNs (45), and YopM might have a similar effect in these cells, although this remains to be shown. Nevertheless, this battery of effectors clearly enables *Yersinia* to avoid PMNs very efficiently. This is seen in the infection experiments presented here, where there were only minor differences in the progression of wt infection between PMN-depleted and undepleted mice.

The avoidance of PMNs by the wt strain was also obvious in the analysis of stable interaction between *Y. pseudotuberculosis* and immune cells during early infection. Here we observed a striking difference between the interaction of wt bacteria with PMNs and that of mutants lacking the antiphagocytic effector YopH or YopE. Although PMNs were present at low numbers in the tissue at day 1 p.i., wt bacteria were not found to interact with these cells. Interaction with PMNs was first observed on day 3 p.i. In contrast, the mutants interacted with PMNs at day 1 p.i. This discrepancy was also obvious at day 3 p.i., when massive PMN infiltration was seen in both wt- and mutant-infected ceca, and the mutants interacted with PMNs much more frequently than the wt did. The discrepancy between the wt and the mutants could not be explained by increased PMN recruitment by the mutants or by an increase in the level of internalization of these mutants, since they, as well as wt bacteria, showed extracellular localization at day 1 p.i. The extracellular localization of *yopH* and *yopE* mutants is in accordance with recently published data showing that live *Y. pseudotuberculosis yopH* and *yopE* mutants are found extracellularly in the spleen (30).

Given the importance of Yop effectors for *Y. pseudotuberculosis* virulence and current knowledge about contact-dependent delivery, we hypothesize that the wt strain interacts transiently with PMNs and that the Yop effectors contribute to its escape. This is supported by the finding that wt bacteria are more capable of reaching deeper sites than the mutant strains, which show a higher fre-

quency of localization and a higher level of PMN interaction in the subepithelial dome area but are rarely found in deeper tissue. The lower invasion capacity of the mutants might be partly responsible for their higher level of PMN interaction. Hence, the Yop effectors enable *Y. pseudotuberculosis* to escape PMNs, whereas the *yop* mutants are captured by these cells in the dome area. This also explains why the mutants can disseminate further and reach the MLNs in the absence of PMNs and shows the importance of these immune cells in restricting bacterial spread.

We also found that depletion of PMNs using the PMN-specific anti-Ly6G antibody had some restrictions involving compensatory mechanisms that complicate analyses at later time points of infection. We observed that already at day 3 p.i., there was no difference in infection efficiency between undepleted and PMN-depleted mice. We suggest that this is due to incomplete depletion of Gr-1^{low} immature PMNs, since it was clear that this population increased in the blood of infected PMN-depleted mice to a level similar to that of Gr-1^{high} mature PMNs in infected undepleted mice. Immature PMNs likely avoid depletion due to their low expression of Ly6G. Our immunohistochemical analysis suggests that Gr-1^{low} immature PMNs, like mature PMNs, are recruited to infected tissues. The possibility that that these cells, when entering the infection site, mature into fully effective PMNs cannot be excluded. In addition, the level of Gr-1^+ F4/80^+ monocytes increased slightly in the blood of infected PMN-depleted mice, and the level of F4/80^+ macrophages increased in infected tissues. Similar results have been observed in the oviducts of PMN-depleted mice infected with *Chlamydia muridarum* (46). Hence, the release of immature PMNs and increased levels of monocytes/macrophages appear to be general effects in anti-Ly6G-treated mice upon infection. Both experimental design and the interpretation of data should take this these phenomena into account.

ACKNOWLEDGMENTS

This work was supported by grants from the Swedish Research Council VR-M (56X-11222-17-6) and the JC Kempe Memorial Foundation.

We thank Kristina Nilsson for constructing the bioluminescent *yopH* mutant and for assistance during mouse infection and Anna von der Marwitz for help with immunohistochemistry and immunofluorescent staining.

REFERENCES

1. **Barnes PD, Bergman MA, Mecsas J, Isberg RR.** 2006. *Yersinia pseudotuberculosis* disseminates directly from a replicating bacterial pool in the intestine. J. Exp. Med. **203:**1591–1601. http://dx.doi.org/10.1084/jem.20060905.
2. **Holmström A, Rosqvist R, Wolf-Watz H, Forsberg A.** 1995. Virulence plasmid-encoded YopK is essential for *Yersinia pseudotuberculosis* to cause systemic infection in mice. Infect. Immun. **63:**2269–2276.
3. **Trcek J, Berschl K, Trulzsch K.** 2010. In vivo analysis of *Yersinia enterocolitica* infection using *luxCDABE*. FEMS Microbiol. Lett. **307:**201–206. http://dx.doi.org/10.1111/j.1574-6968.2010.01983.x.
4. **Simonet M, Richard S, Berche P.** 1990. Electron microscopic evidence for in vivo extracellular localization of *Yersinia pseudotuberculosis* harboring the pYV plasmid. Infect. Immun. **58:**841–845.
5. **Logsdon LK, Mecsas J.** 2006. The proinflammatory response induced by wild-type *Yersinia pseudotuberculosis* infection inhibits survival of *yop* mutants in the gastrointestinal tract and Peyer's patches. Infect. Immun. **74:**1516–1527. http://dx.doi.org/10.1128/IAI.74.3.1516-1527.2006.
6. **Autenrieth IB, Firsching R.** 1996. Penetration of M cells and destruction of Peyer's patches by *Yersinia enterocolitica*: an ultrastructural and histological study. J. Med. Microbiol. **44:**285–294. http://dx.doi.org/10.1099/00222615-44-4-285.
7. **Handley SA, Dube PH, Revell PA, Miller VL.** 2004. Characterization of oral *Yersinia enterocolitica* infection in three different strains of inbred mice. Infect. Immun. **72:**1645–1656. http://dx.doi.org/10.1128/IAI.72.3.1645-1656.2004.
8. **McCoy MW, Marre ML, Lesser CF, Mecsas J.** 2010. The C-terminal tail of *Yersinia pseudotuberculosis* YopM is critical for interacting with RSK1 and for virulence. Infect. Immun. **78:**2584–2598. http://dx.doi.org/10.1128/IAI.00141-10.
9. **Chen J, Harrison DE.** 2002. Quantitative trait loci regulating relative lymphocyte proportions in mouse peripheral blood. Blood **99:**561–566. http://dx.doi.org/10.1182/blood.V99.2.561.
10. **Basu S, Hodgson G, Katz M, Dunn AR.** 2002. Evaluation of role of G-CSF in the production, survival, and release of neutrophils from bone marrow into circulation. Blood **100:**854–861. http://dx.doi.org/10.1182/blood.V100.3.854.
11. **Pillay J, den Braber I, Vrisekoop N, Kwast LM, de Boer RJ, Borghans JA, Tesselaar K, Koenderman L.** 2010. In vivo labeling with ^2H_2O reveals a human neutrophil lifespan of 5.4 days. Blood **116:**625–627. http://dx.doi.org/10.1182/blood-2010-01-259028.
12. **Kolaczkowska E, Kubes P.** 2013. Neutrophil recruitment and function in health and inflammation. Nat. Rev. Immunol. **13:**159–175. http://dx.doi.org/10.1038/nri3399.
13. **Durand EA, Maldonado-Arocho FJ, Castillo C, Walsh RL, Mecsas J.** 2010. The presence of professional phagocytes dictates the number of host cells targeted for Yop translocation during infection. Cell. Microbiol. **12:**1064–1082. http://dx.doi.org/10.1111/j.1462-5822.2010.01451.x.
14. **Conlan JW.** 1997. Critical roles of neutrophils in host defense against experimental systemic infections of mice by *Listeria monocytogenes*, *Salmonella typhimurium*, and *Yersinia enterocolitica*. Infect. Immun. **65:**630–635.
15. **Autenrieth SE, Linzer TR, Hiller C, Keller B, Warnke P, Koberle M, Bohn E, Biedermann T, Buhring HJ, Hammerling GJ, Rammensee H, Autenrieth IB.** 2010. Immune evasion by *Yersinia enterocolitica*: differential targeting of dendritic cell subpopulations in vivo. PLoS Pathog. **6:**e1001212. http://dx.doi.org/10.1371/journal.ppat.1001212.
16. **Köberle M, Klein-Gunther A, Schutz M, Fritz M, Berchtold S, Tolosa E, Autenrieth IB, Bohn E.** 2009. *Yersinia enterocolitica* targets cells of the innate and adaptive immune system by injection of Yops in a mouse infection model. PLoS Pathog. **5:**e1000551. http://dx.doi.org/10.1371/journal.ppat.1000551.
17. **Marketon MM, DePaolo RW, DeBord KL, Jabri B, Schneewind O.** 2005. Plague bacteria target immune cells during infection. Science **309:**1739–1741. http://dx.doi.org/10.1126/science.1114580.
18. **Grosdent N, Maridonneau-Parini I, Sory MP, Cornelis GR.** 2002. Role of Yops and adhesins in resistance of *Yersinia enterocolitica* to phagocytosis. Infect. Immun. **70:**4165–4176. http://dx.doi.org/10.1128/IAI.70.8.4165-4176.2002.
19. **Ruckdeschel K, Roggenkamp A, Schubert S, Heesemann J.** 1996. Differential contribution of *Yersinia enterocolitica* virulence factors to evasion of microbicidal action of neutrophils. Infect. Immun. **64:**724–733.
20. **Thorslund SE, Ermert D, Fahlgren A, Erttmann SF, Nilsson K, Hosseinzadeh A, Urban CF, Fällman M.** 2013. Role of YopK in *Yersinia pseudotuberculosis* resistance against polymorphonuclear leukocyte defense. Infect. Immun. **81:**11–22. http://dx.doi.org/10.1128/IAI.00650-12.
21. **Fahlgren A, Westermark L, Akopyan K, Fällman M.** 2009. Cell type-specific effects of *Yersinia pseudotuberculosis* virulence effectors. Cell. Microbiol. **11:**1750–1767. http://dx.doi.org/10.1111/j.1462-5822.2009.01365.x.
22. **Fällman M, Andersson K, Hakansson S, Magnusson KE, Stendahl O, Wolf-Watz H.** 1995. *Yersinia pseudotuberculosis* inhibits Fc receptor-mediated phagocytosis in J774 cells. Infect. Immun. **63:**3117–3124.
23. **Rosqvist R, Bolin I, Wolf-Watz H.** 1988. Inhibition of phagocytosis in *Yersinia pseudotuberculosis*: a virulence plasmid-encoded ability involving the Yop2b protein. Infect. Immun. **56:**2139–2143.
24. **Rosqvist R, Forsberg A, Rimpilainen M, Bergman T, Wolf-Watz H.** 1990. The cytotoxic protein YopE of *Yersinia* obstructs the primary host defence. Mol. Microbiol. **4:**657–667. http://dx.doi.org/10.1111/j.1365-2958.1990.tb00635.x.
25. **Logsdon LK, Mecsas J.** 2003. Requirement of the *Yersinia pseudotuberculosis* effectors YopH and YopE in colonization and persistence in intestinal and lymph tissues. Infect. Immun. **71:**4595–4607. http://dx.doi.org/10.1128/IAI.71.8.4595-4607.2003.
26. **Hamid N, Gustavsson A, Andersson K, McGee K, Persson C, Rudd CE, Fällman M.** 1999. YopH dephosphorylates Cas and Fyn-binding protein

in macrophages. Microb. Pathog. **27:**231–242. http://dx.doi.org/10.1006/mpat.1999.0301.
27. **Persson C, Carballeira N, Wolf-Watz H, Fällman M.** 1997. The PTPase YopH inhibits uptake of *Yersinia*, tyrosine phosphorylation of p130Cas and FAK, and the associated accumulation of these proteins in peripheral focal adhesions. EMBO J. **16:**2307–2318. http://dx.doi.org/10.1093/emboj/16.9.2307.
28. **Black DS, Bliska JB.** 1997. Identification of p130Cas as a substrate of *Yersinia* YopH (Yop51), a bacterial protein tyrosine phosphatase that translocates into mammalian cells and targets focal adhesions. EMBO J. **16:**2730–2744. http://dx.doi.org/10.1093/emboj/16.10.2730.
29. **Black DS, Marie-Cardine A, Schraven B, Bliska JB.** 2000. The *Yersinia* tyrosine phosphatase YopH targets a novel adhesion-regulated signalling complex in macrophages. Cell. Microbiol. **2:**401–414. http://dx.doi.org/10.1046/j.1462-5822.2000.00061.x.
30. **Rolán HG, Durand EA, Mecsas J.** 2013. Identifying *Yersinia* YopH-targeted signal transduction pathways that impair neutrophil responses during in vivo murine infection. Cell Host Microbe **14:**306–317. http://dx.doi.org/10.1016/j.chom.2013.08.013.
31. **Aili M, Isaksson EL, Hallberg B, Wolf-Watz H, Rosqvist R.** 2006. Functional analysis of the YopE GTPase-activating protein (GAP) activity of *Yersinia pseudotuberculosis*. Cell. Microbiol. **8:**1020–1033. http://dx.doi.org/10.1111/j.1462-5822.2005.00684.x.
32. **Von Pawel-Rammingen U, Telepnev MV, Schmidt G, Aktories K, Wolf-Watz H, Rosqvist R.** 2000. GAP activity of the *Yersinia* YopE cytotoxin specifically targets the Rho pathway: a mechanism for disruption of actin microfilament structure. Mol. Microbiol. **36:**737–748. http://dx.doi.org/10.1046/j.1365-2958.2000.01898.x.
33. **Black DS, Bliska JB.** 2000. The RhoGAP activity of the *Yersinia pseudotuberculosis* cytotoxin YopE is required for antiphagocytic function and virulence. Mol. Microbiol. **37:**515–527. http://dx.doi.org/10.1046/j.1365-2958.2000.02021.x.
34. **Heasman SJ, Ridley AJ.** 2008. Mammalian Rho GTPases: new insights into their functions from in vivo studies. Nat. Rev. Mol. Cell Biol. **9:**690–701. http://dx.doi.org/10.1038/nrm2476.
35. **Daley JM, Thomay AA, Connolly MD, Reichner JS, Albina JE.** 2008. Use of Ly6G-specific monoclonal antibody to deplete neutrophils in mice. J. Leukoc. Biol. **83:**64–70. http://dx.doi.org/10.1189/jlb.0407247.
36. **Tepper RI, Coffman RL, Leder P.** 1992. An eosinophil-dependent mechanism for the antitumor effect of interleukin-4. Science **257:**548–551. http://dx.doi.org/10.1126/science.1636093.
37. **Ye Z, Kerschen EJ, Cohen DA, Kaplan AM, van Rooijen N, Straley SC.** 2009. $Gr1^+$ cells control growth of YopM-negative *Yersinia pestis* during systemic plague. Infect. Immun. **77:**3791–3806. http://dx.doi.org/10.1128/IAI.00284-09.
38. **Ye Z, Uittenbogaard AM, Cohen DA, Kaplan AM, Ambati J, Straley SC.** 2011. Distinct $CCR2^+$ $Gr1^+$ cells control growth of the *Yersinia pestis* Δ*yopM* mutant in liver and spleen during systemic plague. Infect. Immun. **79:**674–687. http://dx.doi.org/10.1128/IAI.00808-10.
39. **Westermark L, Fahlgren A, Fällman M.** 2012. Immune response to diphtheria toxin-mediated depletion complicates the use of the CD11c-DTR(tg) model for studies of bacterial gastrointestinal infections. Microb. Pathog. **53:**154–161. http://dx.doi.org/10.1016/j.micpath.2012.06.004.
40. **Isaksson EL, Aili M, Fahlgren A, Carlsson SE, Rosqvist R, Wolf-Watz H.** 2009. The membrane localization domain is required for intracellular localization and autoregulation of YopE in *Yersinia pseudotuberculosis*. Infect. Immun. **77:**4740–4749. http://dx.doi.org/10.1128/IAI.00333-09.
41. **Thorslund SE, Edgren T, Pettersson J, Nordfelth R, Sellin ME, Ivanova E, Francis MS, Isaksson EL, Wolf-Watz H, Fällman M.** 2011. The RACK1 signaling scaffold protein selectively interacts with *Yersinia pseudotuberculosis* virulence function. PLoS One **6:**e16784. http://dx.doi.org/10.1371/journal.pone.0016784.
42. **Trülzsch K, Sporleder T, Igwe EI, Russmann H, Heesemann J.** 2004. Contribution of the major secreted Yops of *Yersinia enterocolitica* O:8 to pathogenicity in the mouse infection model. Infect. Immun. **72:**5227–5234. http://dx.doi.org/10.1128/IAI.72.9.5227-5234.2004.
43. **Aili M, Isaksson EL, Carlsson SE, Wolf-Watz H, Rosqvist R, Francis MS.** 2008. Regulation of *Yersinia* Yop-effector delivery by translocated YopE. Int. J. Med. Microbiol. **298:**183–192. http://dx.doi.org/10.1016/j.ijmm.2007.04.007.
44. **LaRock CN, Cookson BT.** 2012. The *Yersinia* virulence effector YopM binds caspase-1 to arrest inflammasome assembly and processing. Cell Host Microbe **12:**799–805. http://dx.doi.org/10.1016/j.chom.2012.10.020.
45. **Mankan AK, Dau T, Jenne D, Hornung V.** 2012. The NLRP3/ASC/caspase-1 axis regulates IL-1β processing in neutrophils. Eur. J. Immunol. **42:**710–715. http://dx.doi.org/10.1002/eji.201141921.
46. **Frazer LC, O'Connell CM, Andrews CW, Jr, Zurenski MA, Darville T.** 2011. Enhanced neutrophil longevity and recruitment contribute to the severity of oviduct pathology during *Chlamydia muridarum* infection. Infect. Immun. **79:**4029–4041. http://dx.doi.org/10.1128/IAI.05535-11.